Earth and Planetary Science Letters 371–372 (2013) 103–111

Contents lists available at SciVerse ScienceDirect

Earth and Planetary Science Letters

journal homepage: www.elsevier.com/locate/epsl

Effect of water in depleted mantle on post-spinel transition and implication for 660 km seismic discontinuity

Sujoy Ghosh [a,b,*], Eiji Ohtani [a], Konstantin D. Litasov [a,c,d], Akio Suzuki [a], David Dobson [e], Kenichi Funakoshi [f]

[a] Department of Earth and Planetary Materials Science, Tohoku University, Sendai 980-8578, Japan
[b] Institute of Geochemistry and Petrology, ETH Zürich, CH-8092 Zürich, Switzerland
[c] Novosibirsk State University, Novosibirsk 630090, Russia
[d] V.S. Sobolev Institute of Geology and Mineralogy SB RAS, 630090, Russia
[e] Department of Earth Sciences, University College London, Gower Street, London WC1E 6BT, UK
[f] SPring-8, Japan Synchrotron Radiation Research Institute, Kouto, Japan

ARTICLE INFO

Article history:
Received 13 June 2012
Received in revised form
7 January 2013
Accepted 9 April 2013
Editor: L. Stixrude
Available online 12 May 2013

Keywords:
post-spinel transition
ringwoodite
Mg-perovskite
transition zone
water
660 km discontinuity

ABSTRACT

We have determined the post-spinel transition boundary in anhydrous and hydrous Mg_2SiO_4 in a temperature range from 1173 to 2023 K at 19.3–25.4 GPa using synchrotron *in situ* X-ray diffraction measurements. The phase boundary in Mg_2SiO_4 is located at 22 GPa and 1800 K and 22.1 GPa and 1500 K, which is slightly lower (~0.3–0.5 GPa) than that determined in the previous *in situ* measurements using the same pressure scale [*e.g.* Katsura et al., 2003, Post-spinel transition in Mg_2SiO_4 determined by high *P–T in situ* X-ray diffractometry. Phys. Earth Planet. Inter. 136, 11–24]. The Clapeyron slope of Mg_2SiO_4 was found to be gentle *i.e.* between −0.4 and −0.7 MPa/K, which is also consistent with previous *in situ* measurements, but inconsistent with diamond anvil cell experiments and theoretical estimations. The phase boundary in Mg_2SiO_4+2 wt% H_2O which is relevant to Fe free-depleted harzburgitic composition is located between 23.4 and 23.6 GPa and 1500 K, which shifts the hydrous boundary to the higher pressures relative to anhydrous Mg_2SiO_4 from 1.3 to 1.0 GPa. The result for hydrous Mg_2SiO_4 shows steeper Clapeyron slope between −3.2 and −3.1 MPa/K compared with anhydrous Mg_2SiO_4 and hydrous pyrolite system. The present data suggest that water has a strong influence on 660 km discontinuity and the depressions observed at this boundary in several regions, especially related to subduction zones, can be explained by the presence of water in depleted harzburgite component.

1. Introduction

Water plays an important role in the Earth's evolution and dynamics. The amount of water, even at ppm level, can strongly modify the physical and chemical properties of mantle minerals and rocks. Water can enhance melting (Hirschmann, 2006), affect rheological and transport properties (Chen et al., 1998; Karato, 2006), and also change the phase relations of mantle minerals and rocks and shift their phase boundaries (*e.g.* Wood, 1995; Ohtani et al., 2004). Subducting slabs can transport significant amount of water into the Earth's interior and much of the subducted water can be stored in the mantle transition zone according to recent tomography observations, which suggest that most of the subducted oceanic lithosphere is stagnant above 660 km depth (*e.g.* Fukao et al., 2001, 2009).

The 660 km discontinuity is one of the most important structural boundaries in the Earth's interior and it has been widely accepted to be due to a phase transition in $(Mg,Fe)_2SiO_4$ system (*e.g.*, Green and Ringwood, 1967; Liu, 1976; Ito and Takahashi, 1989). At this boundary, $(Mg,Fe)_2SiO_4$ (γ-spinel or ringwoodite; hereafter Rw) transforms to a mixture of $(Mg,Fe)SiO_3$ (Mg-perovskite; hereafter Pv) and (Mg,Fe)O (ferropericlase). According to seismic observations this boundary is placed at a depth corresponding to a pressure of about 23.6 GPa at 1873 K (Dziewonski and Anderson, 1981; Ita and Stixrude, 1992). This phase boundary is endothermic (Christensen, 1995; Akaogi et al., 1998) and is often called the post-spinel transition (hereafter PST). The 660 km discontinuity is a global feature, but seismological studies suggest that its depth varies considerably in different regions. Short period and vertical waveform data from Fiji–Tonga region and beneath Indian Ocean suggest that the 660-km discontinuity is sharp and flat (*e.g.* Benz and Vidale, 1993;

* Corresponding author at: Institute of Geochemistry and Petrology, ETH Zürich, CH-8092 Zürich, Switzerland. Tel.: +41 44 63 22115; fax: +41 44 63 21636.
E-mail address: sujoy.ghosh@erdw.ethz.ch (S. Ghosh).

0012-821X/$ - see front matter © 2013 Elsevier B.V. All rights reserved.
http://dx.doi.org/10.1016/j.epsl.2013.04.011

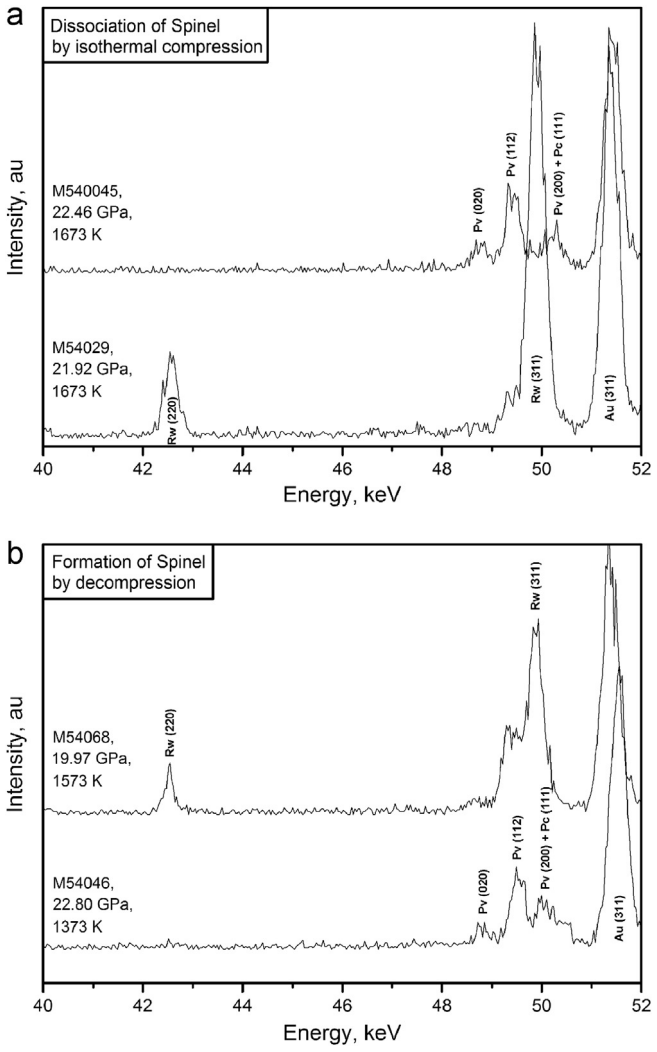

Fig. 1. Representative X-ray diffraction patterns of Mg_2SiO_4 showing (a) dissociation of Rw to Pv+Pc by compression. New Pv peaks e.g. (020), (112) and (200) appear and some Rw peaks *e.g.* (220) and (311) diminish or disappear. (b) Formation of Rw from Pv+Pc by decompression. New Rw peak (220) appears and some Pv peaks *e.g.* (020) diminish or disappear. *Abbreviations:* Rw—ringwoodite; Pv—perovskite; Pc—periclase; Au—gold.

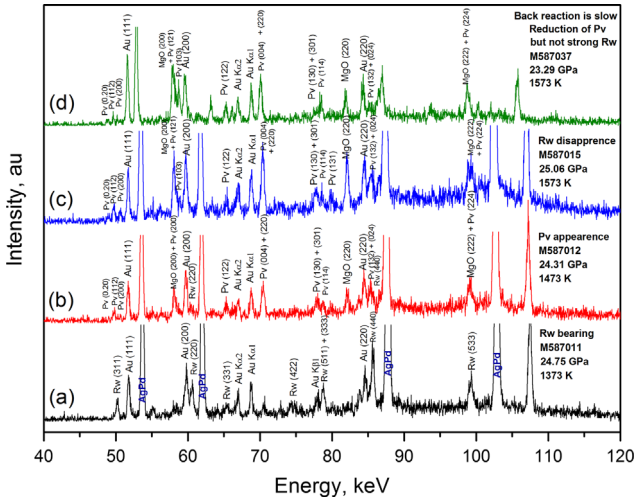

Fig. 2. Representative X-ray diffraction patterns of Mg_2SiO_4+2 wt% H_2O at the indicated *P–T* conditions. Abbreviations are the same as in Fig. 1. Backward transformation of Rw from Pv+Pc is very sluggish and it can be even more sluggish than in dry system either due to growth of large Pv and Pc grains or release of water from the capsule during the experiment.

Yamazaki and Hirahara, 1994). However, comprehensive SS precursor and receiver functions studies in Central Europe and NE China propose that the discontinuity is depressed by 30–70 km or shows significant variations over short spatial wavelengths (*e.g.* Petersen et al., 1993; Flanagan and Shearer, 1998; Helffrich, 2000; Gu and Dziewonski, 2002; Li and Yuan, 2003; Hetényi et al., 2009; Lombardi et al., 2009; Wang and Niu, 2010; Cornwell et al., 2011). The most often mentioned effect to explain these seismic observations is the lateral variation or gradient in temperature (*e.g.* Shearer, 2000) beneath 660 km (Helffrich, 2000), and only a few studies evoke chemical changes as well (*e.g.* Cornwell et al., 2011 and references therein).

To correlate 660 km seismic discontinuity, it is important to know the precise pressure–temperature conditions for the PST (see Ohtani and Litasov (2006) for review). Recent *in situ* X-ray diffraction measurements on pure Mg_2SiO_4 (Irifune et al., 1998; Katsura et al., 2003; Fei et al., 2004b) and a pyrolitic composition (Litasov et al., 2005a) using multianvil technique suggest that the boundary is located at lower pressures than the actual pressure of 660 km discontinuity (~23.6 GPa) and shows a gentle negative Clapeyron slope ranging from −0.4 to −1.3 MPa/K (*e.g.* Katsura et al., 2003; Fei et al., 2004b; Litasov et al., 2005a) such that large variations in the depth of 660 km discontinuity cannot be explained by a temperature effect only. Conversely, laser heating diamond anvil cell (LHDAC) experiments (Chudinovskikh and Boehler, 2001; Shim et al., 2001) and first-principles estimations for Mg_2SiO_4 (Yu et al., 2007), in which the density function theory (DFT) was adopted, show reasonable agreement with pressure and expected Clapeyron slope of the 660 km discontinuity. These latter data support original determination of the depth and Clapeyron slope for the post-spinel transition by Ito and Takahashi (1989) using laboratory multianvil experiments. However, it is important to note that LHDAC experiments may give a large uncertainty in temperature measurements and be influenced by kinetic effects (Li and Jeanloz, 1987). Furthermore, DFT simulations tend to have relatively large errors in transition pressures for non-isochemical transitions at finite temperature.

It was shown that water and other compositional variations might affect the depth and thickness of the 660 km discontinuity (*e.g.* Litasov et al., 2005b). Rw is the most important phase at the lower part of the transition zone from 520 to 660 km depth (Ringwood, 1975). It can incorporate a large amount of hydrogen in its structure (up to 3.0 wt% H_2O) (*e.g.* Kohlstedt et al., 1996; Bolfan-Casanova et al., 2000; Ohtani et al., 2000). In contrast, the most relevant results to date suggest that Mg-Pv and periclase (hereafter Pc) have very low hydrogen solubility (*e.g.* Bolfan-Casanova et al., 2002, 2003; Litasov et al., 2003; Litasov, 2010). Based on thermodynamic relations, hydrogen incorporation into Rw can expand its stability field to higher pressures relative to anhydrous system (Higo et al., 2001; Litasov et al., 2005b; Ohtani, 2005; Ohtani and Litasov, 2006).

The effect of water on the 660 km discontinuity has not been studied extensively. Higo et al. (2001) first noted the shift of the post-spinel phase boundary in Mg_2SiO_4 under hydrous condition based on laboratory experiments and thereafter Litasov et al. (2005b) have studied the post-spinel transition in a hydrous pyrolite system using *in situ* technique and observed the shift of this boundary ~0.6 GPa toward higher pressure compared to anhydrous pyrolite at 1473 K. However, the Clayperon slope was poorly constrained due to restricted temperature interval of measurements. Besides, it is difficult to distinguish the effect of water from a combined effect of other components in the system, such as Al, Fe, and Ca. Therefore, to distinguish the effect of water

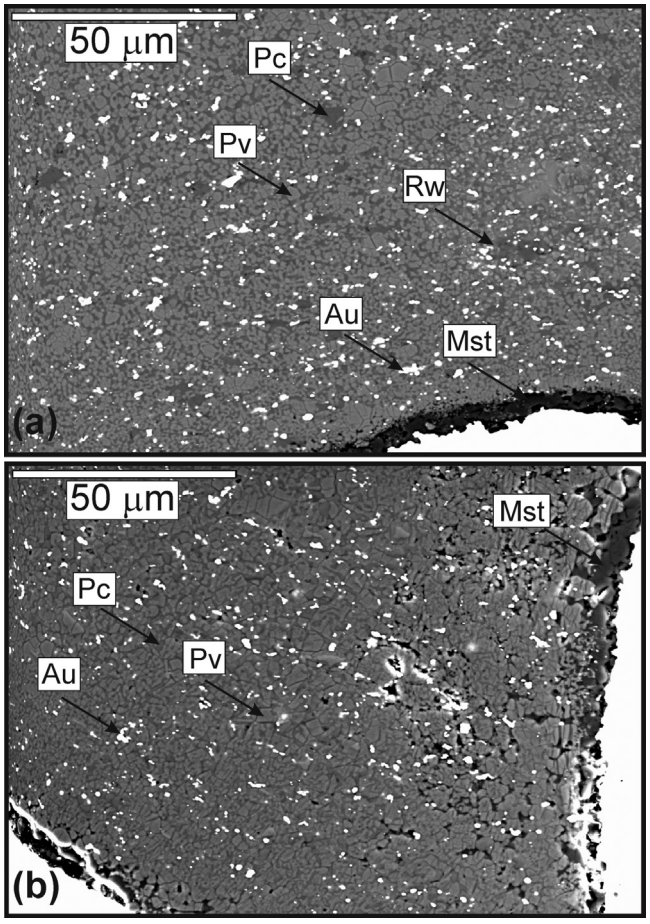

Fig. 3. (a) Back-scattered electron images of the sample (M587) quenched from 1573 K and 23.41 GPa. (b) Back-scattered electron images of the sample (S1913) quenched from 1673 K and 24.42 GPa. Small amount of magnesite was present at one corner of the capsule in both runs mainly because commercial brucite absorbs CO_2 from the atmosphere that cannot be dried off and which typically causes formation of magnesite in experiments. *Abbreviations:* Rw—ringwoodite; Pv—perovskite; Pc—periclase; Au—gold; Mst—magnesite.

on the post-spinel transition boundary, one needs to study the water-bearing Mg_2SiO_4 system.

In this study, we examine the post-spinel transition boundary in Mg_2SiO_4 at 19.3–24.1 GPa and temperature up to 2023 K by means of *in situ* X-ray diffraction in a multi-anvil apparatus and present new data on the post-spinel transition boundary in Mg_2SiO_4+2 wt% H_2O at 21.5–25.4 GPa and temperature up to 1673 K. Based on these data, we illustrate the influence of water on the post-spinel transition and interpret the result with respect to the 660-km seismic discontinuity and its variations with depth.

2. Experimental procedure

All *in situ* X-ray diffraction experiments were carried out at synchrotron radiation facility 'SPring-8', Hyogo prefecture, Japan. We used Kawai-type multi-anvil apparatuses, '*SPEED-1500*' and '*SPEED-Mk.II*', installed at a bending magnet beam line BL04B1. Energy-dispersive X-ray diffractometry was conducted with a horizontal goniometer using white X-rays. Incident X-ray was collimated to form a thin beam with the horizontal and vertical thicknesses of 0.05 and 0.2 mm, respectively, by tungsten carbide slits to direct the samples through pyrophyllite gaskets. A Ge-solid state detector was used and connected to 4096-channel analyzer, which was calibrated by using characteristic X-rays of Cu, Mo, Ag, Ta, Pt, Au, and Pb. Exposure times were 300–500 s. The diffraction angle (2θ) was $\sim$6.0°. The diffraction angles were calibrated before compression for each run using d-values of X-ray diffraction peaks and unit cell parameters of gold (a_0=4.0786 Å). The diffraction angles were determined with uncertainty of less than 0.0005°.

The starting material for dry runs was synthetic crystals of forsterite representing Mg_2SiO_4 mixed with the Au-pressure marker at 20:1 by weight. In the wet runs we used a mixture of forsterite, enstatite, and brucite $Mg(OH)_2$. Water (2 wt%) was added as $Mg(OH)_2$ in the starting material adjusting the proportion of MgO to the stoichiometry of forsterite. Co-doped MgO was used as a pressure medium for low temperature experiments (up to 1773 K) whereas Cr-doped MgO was used for higher temperature runs (above 1773 K). We used a cylindrical $LaCrO_3$ heater as a furnace assembly. Graphite and thin-walled AgPd capsules were used as a sample container in anhydrous and hydrous systems, respectively, which were isolated from the molybdenum electrodes and heater by MgO insulators. Temperature was measured by a $W_{97}Re_3$–$W_{75}Re_{25}$ thermocouple with a junction located at nearly the same position as an X-ray path through the sample. The truncated edge length (TEL) of the WC anvil was 3.0 mm. The design of the cell assembly was similar to that given in Litasov et al. (2005a) for TEL 2.0 mm with adopted proportions of the cell parts. The temperature gradient in the sample capsule was inferred to be about $\pm$50 °C (Kubo et al., 2002). The effect of pressure on the emf of thermocouple was ignored during the experiments.

For each experiment the cell assembly was first compressed to the desired press load at ambient temperature and then heated gradually to the target temperature. This temperature was maintained before obtaining the clear Rw- or Pv-bearing pattern. Thereafter, while continuously taking the diffraction patterns, temperature and the press load were increased and decreased, following complex *PT*-paths.

During the experiments the generated pressure at high temperature was estimated from the unit cell volume of gold using equation of state (EOS) by Tsuchiya (2003). We also placed the phase boundary using other EOS for Au in Supplementary Tables 1 and 2 and Figs. 4 and 5 in anhydrous and hydrous Mg_2SiO_4. Typically, four diffraction lines (111), (200), (220), and (311) of Au were used to calculate pressure. Uncertainty of unit cell volume of Au determined by the least squares method gives 0.1–0.3 GPa uncertainties in pressure. It was possible to use

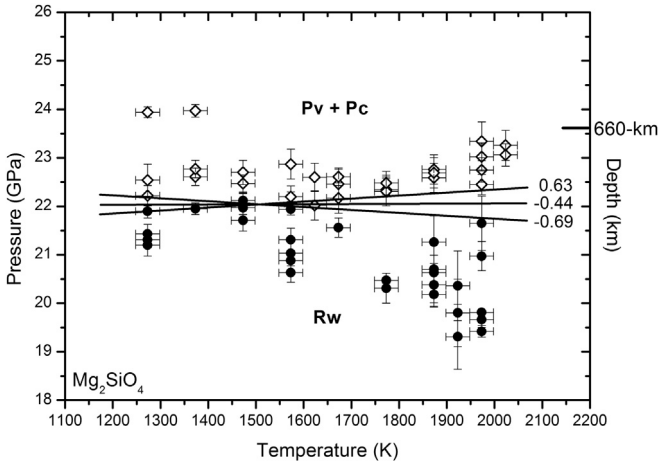

Fig. 4. Phase diagram of Mg_2SiO_4 based on Au pressure scale by Tsuchiya (2003). The solid black circle and solid white diamond represent data points which represent increase of Rw and/or decrease of Pv+Pc and decrease of Rw and/or increase of Pv+Pc, respectively. The solid black lines show the possible location of the post-spinel transition boundary in Mg_2SiO_4 with the Clapeyron slope between −0.69 and 0.63 MPa/K and the middle value is −0.44 MPa/K.

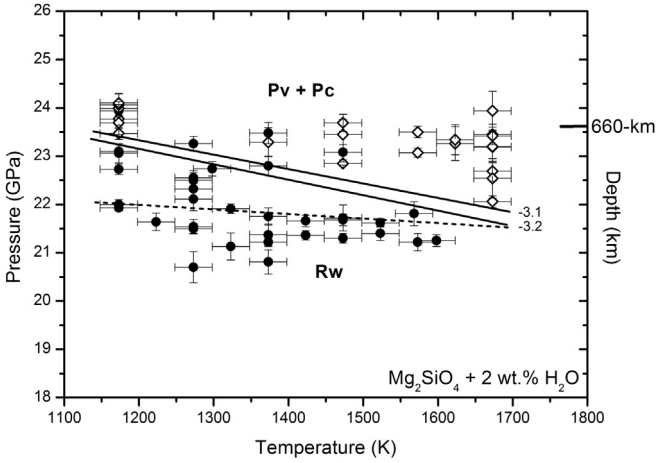

Fig. 5. Phase diagram of Mg_2SiO_4+2 wt% H_2O based on Au pressure scale by Tsuchiya (2003). The symbols are the same as in Fig. 4. The solid black lines are the upper and lower boundaries of the PST boundary in hydrous Mg_2SiO_4 with the Clapeyron slope between −3.2 and −3.1 MPa/K. PST boundary in Mg_2SiO_4 determined by this study (Au pressure scale by Tsuchiya (2003); dashed line) was plotted for comparison.

MgO as a pressure marker; however, MgO peaks were usually weak with high FWHM (in Pv-bearing patterns) or not observed (in Rw-bearing patterns) and showed a large uncertainty in determined pressures.

It is difficult to dissociate Rw from Pv and Pc in anhydrous system (Katsura et al., 2003) and due to this problem we used the following procedure to define the phase boundary of post-spinel in anhydrous and hydrous systems. In the anhydrous run, the post-spinel transition boundary is defined when at least two Rw peaks could be observed and some perovskite peaks should be disappeared or diminished. In hydrous run, post-spinel transition boundary is defined based on formation of Pv and Pc and dissociation of Rw (forward reaction). Although we have tried the backward reaction (formation of Rw by isothermal decompression) in this system (M587 and M687), we realized that the back transformation from Pv+Pc is very sluggish and it can be even more sluggish than in dry system perhaps due to growth of large Pv and Pc grains. Recovered samples were polished and examined by an electron microprobe (JEOL Superprobe JXA-8800) at Tohoku University, and confirmed the results of *in situ* X-ray observations. An acceleration voltage of 15 kV and a 10–15 nA specimen current were used for the analyses.

3. Experimental results

We have carried out 4 experiments at different *P–T* conditions to constrain the post-spinel transition boundary in anhydrous Mg_2SiO_4 tightly. The phase relations were determined at pressures between 19.3 and 24.1 GPa and temperatures up to 2023 K. We also conducted 11 experiments in Mg_2SiO_4+2 wt% H_2O system at pressures of 21.5–25.7 GPa and temperatures up to 1673 K. During each experiment at the final run conditions where diffraction peaks of Rw and/or Pv+Pc either disappear (or diminishing) or appear (or increasing) in dry and hydrous Mg_2SiO_4 systems, the press load and temperature were kept same between 10 and 90 min.

3.1. Dry Mg_2SiO_4

P–T diagram of post-spinel transition boundary in Mg_2SiO_4 without water based on Au scale by Tsuchiya (2003) is plotted in Fig. 4 and summarized in Supplementary Table 1.

In run M619, Rw was present at 21.9 GPa and 1273 K. With increasing temperature we observed the appearance of Pv at 22.3 GPa and 1773 K; further we observed complete disappearance of Rw and strong growth of Pv and Pc peaks at 1873 K and 22.6 GPa. Then temperature was increased up to 2023 K at 23.3 GPa, and clear diffraction patterns of Pv and Pc were obtained. Finally we decreased the temperature up to 1973 K and did isothermal decompression and observed fast growth of Rw at 21.7 GPa and 1973 K. Pv and Pc peaks diminished and Rw peaks grew rapidly when temperature was decreased from 1973 to 1873 K at 20.7 GPa.

In run S1771, pressure was increased to 24.9 GPa at room temperature and Rw peaks were observed with Pv and Pc at 23.9 GPa and 1273 K and with increasing temperature we observed strong peaks of Pv and Pc at 1373 K. With time we observed rapid growth of Pv and Pc and diminishing of Rw peaks. We decreased pressure and observed growth of Rw peaks at 20.9 GPa and 1273 K. At 21.8 GPa and 1373 K some Pv and Pc peaks disappeared. Then, we gradually increased the temperature to 1573 K, and we found that Rw peaks were diminishing and that there was growth of Pv peaks, suggesting that we are very close to the boundary. We further increased the temperature up to 1673 K and a clear diffraction pattern of Rw was observed at 21.5 GPa and 1673 K. With time Rw peaks were stronger and Pv and Pc were diminishing. We again decreased the temperature to 1273 K and some new Pv and Pc peaks appeared at 22.2 GPa. When we again increased the temperature to 1373 K, Pv and Pc peaks were strong and Rw peaks were diminishing. Further increase of temperature to 1473 K showed diminishing of Pv and Pc peaks and growth of Rw peaks at 21.7 GPa and 1473 K.

In run M540, pressure was increased to 22.1 GPa at ambient temperature and temperature was increased to 1273 K. Rw was observed at 21.3 GPa and 1273 K. By compression Rw was dissociated to Pv+Pc at 22.2 GPa and 1573 K (Fig. 1a). With decreasing the pressure, Rw peaks appeared and some Pv peaks diminished or disappeared at 21.0 GPa and 1573 K (Fig. 1b).

In run S1872, pressure was increased to 21 GPa at ambient temperature, and temperature was directly increased to 1773 K, then, gradually increased to 1973 K, and held at this temperature and 19.3 GPa for 20 min. We observed only Rw peaks and no Pv peaks in this run.

3.2. Mg_2SiO_4+2 wt% H_2O

Phase diagram of Mg_2SiO_4+2 wt% H_2O based on Au scale by Tsuchiya (2003) is plotted in Fig. 5 and summarized in Supplementary Table 2.

X-ray diffraction patterns observed in run M587 are shown in Fig. 2. Pressure was increased initially up to 23.5 GPa at ambient temperature, and then temperature was increased to 1173 K. A clear diffraction pattern of Rw was present at 24.2 GPa and 1173 K. We further increased the temperature to 1373 K and still strong Rw peaks were present at 24.8 GPa (Fig. 2a). With increasing temperature we observed appearance of Pv and Pc peaks at 24.4 GPa and 1473 K (Fig. 2b). Following further increase of temperature, we observed strong growth of all the peaks of Pv and Pc and disappearance of Rw peaks at 25.1 GPa and 1573 K (Fig. 2c). We then used isothermal decompression in order to obtain Rw-bearing patterns again, but no Rw peaks were observed at 23.3 GPa and 1573 K (Fig. 2d) (see discussion).

In run M519, pressure was increased to 21.9 GPa at room temperature, and then we gradually increased temperature up to 1473 K at 23.3–24.4 GPa. Rw was always observed and no Pv+Pc was observed in these conditions. No phase transformation between Rw and Pv and Pc was observed in this run. We cannot identify the wet boundary in this run. If we plot the Rw peaks in

Fig. 5, then the post-spinel phase boundary in hydrous Mg_2SiO_4 is located at little higher pressure.

In M589, pressure was increased to 25.3 GPa at ambient temperature. Temperature was increased to 1173 K at 23.8 GPa to obtain Rw. The sample was heated to 1473 K at 24.1 GPa, and the peaks of Pv were obtained. At constant load and increasing temperature to 1673 K, the peaks of Pv and Pc became strong with time. EPMA analysis of the quenched sample confirmed that the final product was composed of mostly Pv+Pc with minor amount of Rw (Fig. 3a).

In M670, we increased the pressure to 25.8 GPa at ambient temperature. At first strong Rw peaks appeared at 25.3 GPa and 1173 K and after heating for a long time at the condition close to ~25.3 GPa and 1173 K we observed transformation from Rw to Pv and Pc at 25.2 GPa and 1173 K. After heating for a long time only strong peaks of Pv and Pc were present.

In run S1913, we observed only Pv and Pc peaks at pressure between 24.4 and 24.7 GPa and 1673 K. BSE image shows that the quenched sample is composed of Pv+Pc (Fig. 3b). In run M625, we also observed strong Pv and Pc peaks at pressure between 25.3 and 25.4 GPa at 1673 K. We decreased the temperature at room temperature and decompress the sample up to 20.6 GPa and we again rapidly increased the pressure and temperature and collected the patterns at 25.0 GPa and 1473 K (M625010) but we only observed strong Pv and Pc peaks in this run.

In run M672, pressure was increased up to 24.7 GPa at ambient temperature and with increasing temperature Rw peaks were observed at 24.9 GPa and 1173 K. After 5 min of heating at the same condition Pv and Pc peaks appeared. After heating for a long time at the same condition, Rw peaks disappeared and Pv and Pc peaks were strong at 24.7 GPa and 1173 K.

In run M687, pressure was increased to 24.9 GPa at room temperature and with increased temperature strong Rw peaks were observed at 24.4 GPa and 1173 K. After 30 min at the same *P–T* conditions Rw peaks started to decrease and Pv and Pc peaks appeared and started to grow with time. In this run, we did the isothermal decompression but we could not form Rw only because we realized that back transformation from Pv+Pc is very sluggish and it can be even more sluggish than in dry system either due to growth of large Pv and Pc grains or release of water from the capsule during the experiment. Therefore we have not included the data points of this experiment in Fig. 5.

3.3. Unit cell volume of ringwoodite: semi-quantitative method to determine the water content

Unit cell volumes of Rw in dry and hydrous Mg_2SiO_4 samples were measured at temperatures from 1173 to 1373 K and pressure from 15 to 24 GPa. Unit cell volumes of dry and hydrous Rw are plotted as a function of pressure in Fig. 1 (Supplementary content). We used the following lines to calculate the unit cell volume at $2\theta = 6.0^\circ$: (220), (311), (400), (422) and (511) for dry Rw and (311), (400), (422) and (511) for hydrous Rw. Unit cell volumes of hydrous Rw between 1173 and 1373 K clearly show slightly higher volume than those calculated for anhydrous Rw at the same temperatures. However, precision of volume determination is not enough to constrain quantitative suggestions about H_2O contents. The calculated volume data in both dry and hydrous runs are scattered mainly due to poor diffraction from Rw in hydrous samples, and many peaks are intersected with Au, AgPd, Pv and Pc peaks. The precision of volume measurements is about ± 0.4 A^3, which corresponds to 0.2%. The difference between V_{hy} and V_{dry} is about 0.8–1 A^3 at 1273–1373 K and 22–24 GPa, which is 0.2–0.25%—the value comparable with volume measurement error. These uncertainties are comparable with measurements by Katsura et al. (2004a, 2004b) for single-phase anhydrous Rw with MgO capsule. Above 1373 K, we did not calculate the unit cell volume of hydrous Rw mainly because grain growth problem reduced the number of observed peaks at these conditions. However, we note that the wet Rw samples are consistently larger than dry samples, by approximately the amount required for the presence of ~0.7% of water in the Rw.

4. Discussion and conclusions

4.1. Comparison with previous studies on post-spinel transition

4.1.1. Mg_2SiO_4

We compared our results with previous studies on Mg_2SiO_4, $(Mg,Fe)_2SiO_4$ and pyrolite compositions (see Fig. 6) (Ito and Takahashi, 1989; Akaogi et al., 1989; Irifune et al., 1998; Shim et al., 2001; Chudinovskikh and Boehler, 2001; Katsura et al., 2003; Fei et al., 2004b; Litasov et al., 2005a; Yu et al., 2007). It was found that the post-spinel transition boundary and its Clapeyron slope vary widely in different studies and are not consistent with each other (see Ohtani and Litasov (2006), for review). Several methods have been used to determine the transition of post-spinel boundary, which are quench laboratory experiments using multianvil apparatus (*e.g.* Ito and Takahashi, 1989; Ishii et al., 2011), thermodynamic and theoretical calculations (*e.g.* Akaogi et al., 1989; Yu et al., 2007), *in situ* X-ray diffraction measurements using multianvil technique (*e.g.* Irifune et al., 1998; Katsura et al., 2003; Fei et al., 2004b) and *in situ* LHDAC experiments (*e.g.* Chudinovskikh and Boehler, 2001; Shim et al., 2001). In all these methods, the measured and calculated boundaries of post-spinel transition

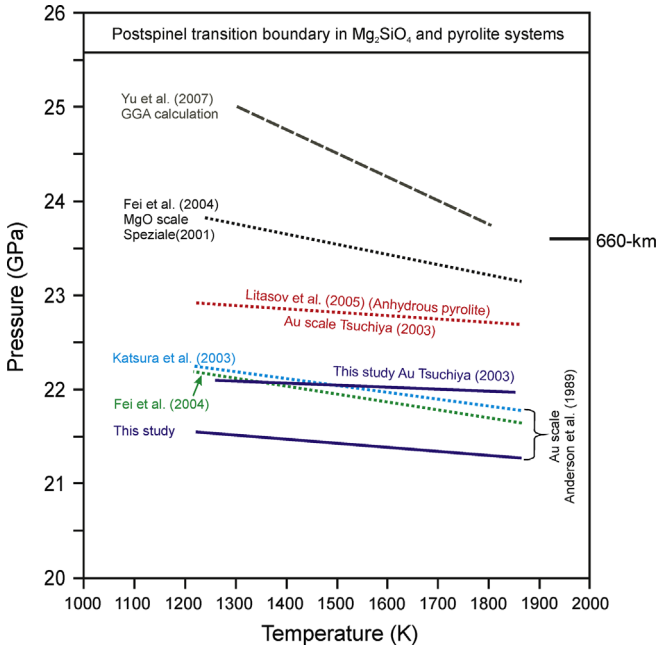

Fig. 6. Post-spinel transition boundary in Mg_2SiO_4 using Au pressure scale (Tsuchiya, 2003) in this study (blue solid line) and compared with previous results in Mg_2SiO_4 and pyrolite systems using different pressure scales. At the left hand side post-spinel transition in Mg_2SiO_4 in this study (blue solid line) is compared with previous results [Katsura et al., 2003 (blue dashed line); Fei et al., 2004b (green dashed line)] in Au scale by Anderson et al. (1989). Post-spinel transition boundary in Mg_2SiO_4 using MgO scale (Speziale et al., 2001) by Fei et al. (2004b) (grey dashed line) and using GGA calculation by Yu et al. (2007) (black dashed line) is also plotted. Post-spinel transition boundary is plotted in pyrolite composition using Au scale (Tsuchiya, 2003) by Litasov et al. (2005a) (red dashed line). (For interpretation of the references to color in this figure legend, the reader is referred to the web version of this article.)

in Mg_2SiO_4 are located in the ranges from 21 to 23.5 GPa at 1500–1900 K.

Using Fo_{90} composition and quench technique in multianvil apparatus, Ito and Takahashi (1989) located the post-spinel transition boundary at 23 GPa and 1900 K with a steep Clapeyron slope of −3.0 MPa/K. First *in situ* measurements by Irifune et al. (1998) for this boundary in Mg_2SiO_4 using the Au pressure scale (Anderson et al., 1989) found essentially the same negative Clapeyron slope as observed by Ito and Takahashi (1989). Since they used Au pressure scale by Anderson et al. (1989), the phase boundary was placed more than 2 GPa lower than pressure of the 660 km discontinuity. Later LHDAC experiments and improved technique in multianvil press have confirmed that this boundary is placed at higher pressures (Chudinovskikh and Boehler, 2001; Shim et al., 2001; Katsura et al., 2003; Fei et al., 2004b). Katsura et al. (2003) have shown that the post-spinel transition is very sluggish, so that complete transformation from Rw to Pv and Pc is difficult especially at high temperature (~2000 K). The phase boundary of the post-spinel transition determined in the present study using Au scale by Tsuchiya (2003) is slightly lower (~0.3–0.5 GPa) than that by Katsura et al. (2003) and Fei et al. (2004b) recalculated to the same pressure scale. This minor discrepancy is almost inside the possible uncertainties and may be explained by differences in cell assembly configurations. Fei et al. (2004a) have discussed the accuracy of the different pressure scales and observed that the MgO pressure scale (Speziale et al., 2001) may be more reliable compared to Au, Pt and NaCl; it places the post-spinel transition boundary in Mg_2SiO_4 at 23.6 GPa at 1673 K, which is close to the pressure of 660 km discontinuity. In the present study the transition pressure based on Au pressure scale by Tsuchiya (2003) is about 1.5 GPa lower than the pressure at 660 km (Fig. 6).

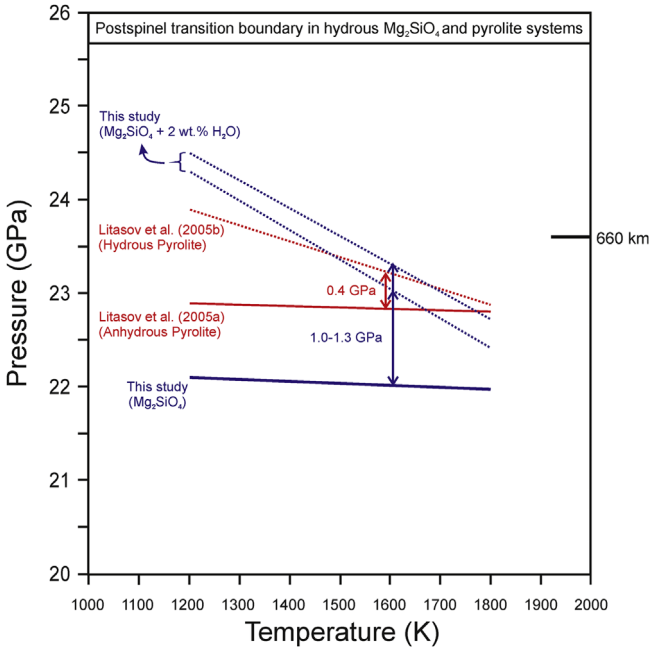

Fig. 7. Post-spinel transition boundary in Mg_2SiO_4+2 wt% H_2O using Au pressure scale (Tsuchiya, 2003) in this study and compared with previous results in pyrolite composition by Litasov et al. (2005b). The solid and dashed blue lines are the post-spinel transition boundary in Mg_2SiO_4 and Mg_2SiO_4+2 wt% H_2O using Au scale (Tsuchiya, 2003) in this study. The solid and dashed red lines are the boundary in anhydrous and hydrous pyrolite using the Anderson Au scale by Litasov et al. (2005a, 2005b). Mg_2SiO_4+2 wt% H_2O shifts the PST boundary to 1.0–1.3 GPa at 1600 K (this study) compared to 0.4 GPa at 1600 K in hydrous pyrolite system (Litasov et al., 2005b). (For interpretation of the references to color in this figure legend, the reader is referred to the web version of this article.)

4.1.2. Mg_2SiO_4+2 wt% H_2O

In order to constrain the effect of water on the post-spinel transition boundary, we plotted data on the post-spinel transition in Mg_2SiO_4+2 wt% H_2O along with those in pure Mg_2SiO_4 and anhydrous and hydrous pyrolite (Fig. 7). Litasov et al. (2005b) have studied the post-spinel transition in hydrous pyrolite (with 2 wt% H_2O) and clearly observed that the phase boundary is shifted to higher pressure by 0.4 GPa compared to anhydrous pyrolite at 1600 K. In the present study, there is an invariant point (but not a loop) of ringwoodite+perovskite+periclase with some finite width at the transition marking the upper/lower mantle boundary. Nevertheless, the width of the reaction band is unknown and our experiments do not allow to constrain this feature. We observe which phase grows but cannot determine if the phase that decreases in modal proportions is still stable or not. According to the present experiment, the phase boundary of the post-spinel transition in hydrous Mg_2SiO_4 is shifted to higher pressure from 1.0 to 1.3 GPa at 1600 K, which is equal to ~30–40 km depth. We could find that the pressure shift of the post-spinel boundary in the present study is nearly three times larger relative to hydrous pyrolite (Litasov et al., 2005b). It is known that Fe shifts the post-spinel transition boundary to lower pressure by 2.0–2.5 GPa in dry Fo_{90} system compare to the pure Mg_2SiO_4 system (Ito and Takahashi, 1989). So, it would be expected that Fe will reduce the transition pressure in the wet systems too. In contrast, adding Al should shift the stability of the lower pressure assemblage to higher pressure. Wood and Rubie (1996) studied the Fe/Mg partitioning between Pv, magnesiowüstite, and Rw and observed that in peridotitic mantle, Fe strongly partitions into Al_2O_3-rich Pv (Fe#=0.11) which is the same as magnesiowustite (Fe#=0.10). Weidner and Wang (1998) argued that a slight increase in Al_2O_3 content can shift the post-spinel transition to higher pressure. Thus, the destabilizing effect of FeO counteracts the stabilizing effect of Al_2O_3 on the dry and wet pyrolite systems.

4.2. Depth of the post-spinel transition

Seismological studies (Flanagan and Shearer, 1998; Gu and Dziewonski, 2002) show that the global average for the depth of 660 km discontinuity varies between 647 and 654 km. Based on global data set of receiver function, Andrews and Deuss (2008) pointed out that the 660 km discontinuity stabilizes at higher depth and shows asymmetric peaks in a global scale and maximum peak of the discontinuity is 600–800 km. Most *in situ* multianvil measurements on Mg_2SiO_4 (Katsura et al., 2003; Fei et al., 2004b; this study) and a pyrolite composition (Litasov et al. 2005a) suggest that the post-spinel transition boundary should be located slightly or even significantly shallower than 660 km as far as presently available pressure scales are used. Litasov et al. (2005a) placed this boundary at 22.6 GPa and 1800 K in anhydrous pyrolite composition using the Tsuchiya Au scale. Using MgO scale by Speziale et al. (2001), Fei et al. (2004b) located this boundary at 23.6 GPa and 1673 K, which is close to the pressure estimated at 660 km (~23.5 GPa). Diamond anvil cell experiments by Shim et al. (2001) and Chudinovskikh and Boehler (2001) have shown that the transition depth agrees well with the 660 km discontinuity for Mg_2SiO_4 system. These results are supported by recent first-principles calculations (Yu et al., 2007).

Recent mineral physics and seismological data provide comprehensive information about the possible existence of water in the transition zone which supports the conceptual models (hydrous transition zone by Ohtani et al. (2004); water filter model by Bercovici and Karato (2003)). Recent electrical conductivity measurement by Huang et al. (2005) suggested that water

content in the transition zone may be ~0.1–0.2 wt%. If sufficient water is present in the transition zone then depression of the 660 km boundary should be maximal. Our experimental data suggest that a shift of this boundary by adding water can be up to ~1.3 GPa, which corresponds to 40 km deeper in depth. To date, there are several regions, where such depressions have been identified, *e.g.* beneath the Ethiopian rift and Northeast China (Cornwell et al., 2011; Kuritani et al., 2011).

4.3. The Clapeyron slope of the post-spinel transition

Early seismological and thermodynamic models considered that 660 km discontinuity is sharp *i.e.* less than 5 km (*e.g.* Benz and Vidale, 1993; Yamazaki and Hirahara, 1994) with a steep negative Clapeyron slope (−2.9 MPa/K, Bina and Helffrich, 1994) which has profound effect on mantle dynamics and is related with layered or whole mantle convection (Hofmann 1997; Schubert et al., 2001; Tackley et al., 1993). Based on a regional tomography model, Lebedev et al. (2002) found that the seismologically inferred Clapeyron slope agrees with thermodynamics calculations in olivine (Bina and Helffrich, 1994).

Akaogi et al. (1998) have calculated the phase boundary of the post-spinel transition using calorimetric calculations and have shown a steep negative Clapeyron slope (-3 ± 1 MPa/K). Recently, Yu et al. (2007) reported the results of the first principle calculations on the post-spinel transition in Mg_2SiO_4 using quasi-harmonic free energy computations with local density (LDA) and generalized gradient (GGA) approximation. Their GGA approximation results suggest that Rw dissociates to Pv and Pc at 23.2 GPa and 1900 K with a steep Clapeyron slope (−2.9 MPa/K). The estimated slope from first principle study is consistent with the seismological observations (*e.g.* Lebedev et al., 2002). The Clapeyron slope in the present study in Mg_2SiO_4 is much gentler than the theoretical (Yu et al., 2007) and quench experimental results (Ito and Takahashi, 1989). However, we have found the same gentle Clapeyron slope in the present study compared with previous *in situ* studies in Mg_2SiO_4 (Katsura et al., 2003; Fei et al., 2004b). The quench experiments by Ito and Takahashi (1989) found the Clapeyron slope of −3.0 MPa/K, which is significantly smaller than those obtained by recent *in situ* X-ray diffraction experiments (this study: from −0.43 to −0.85 MPa/K; Katsura et al. (2003): from −2.0 to −0.4 MPa/K; Fei et al. (2004b); −1.3 MPa/K; Litasov et al. (2005a): from −0.8 to −0.2 MPa/K; Fig. 6). In the present study, we constrain the upper and lower boundaries of the Clapeyron slope in Mg_2SiO_4+2 wt% H_2O between −3.2 and −3.1 MPa/K. In contrast to the *in situ* studies of anhydrous systems the Clapeyron slope of the PST in water-bearing Mg_2SiO_4 and pyrolite is significantly steeper from −3.2 to −3.1 MPa/K in Mg_2SiO_4 in the present work and −2.2 MPa/K in hydrous pyrolite (Litasov et al., 2005b).

4.4. Geophysical implications

It is important and informative to consider the relative effect of water and temperature on the post-spinel phase transition. The dry system considered in this study has a very gentle Clapeyron slope (*i.e.* −0.43 MPa/K) such that a change in temperature of 473 K only changes the pressure of the phase boundary by ~0.09 GPa. Water on the other hand appears to have a much larger effect. We have not measured the water content of our samples in the present study, but the water content of the wet charge should have been sufficient for the Rw to be saturated (~1 wt% water in $(Mg, Fe)_2SiO_4$ Rw at 1673 K; Smyth et al., 2003; ~1 wt% water in Mg_2SiO_4 Rw at 1873 K; Ohtani et al., 2000) and so we assume this to be the case in the following discussion. At 1873 K, which is a reasonable temperature for the mantle at 660 km depth (Katsura et al., 2004a, 2004b; Katsura et al., 2010), the difference between the dry and water-saturated phase boundaries in the Mg_2SiO_4 system studied here is over 1 GPa. In order, therefore, to change the pressure of the PST by 0.09 GPa (equivalent to a temperature change of 473 K) at a constant temperature of 1873 K the water content in the Rw must change by only 0.09 wt%, assuming a linear dependence of the equilibrium pressure on the water content. The effect of water on the equilibrium phase boundary is also larger than the effect of changing the bulk composition from the simple magnesian end-member studied here (*i.e.* is close to harzburgitic composition) to that of pyrolite studied by Litasov et al. (2005b) (Fig. 7). The effect of water is even larger at lower temperatures since a Clapeyron slope in the wet system is more strongly negative compared to that in the dry system. We would suggest therefore that the topography on the 660 km discontinuity could be due to variation of the water content in the transition zone.

Recent combined geomagnetic and laboratory electrical conductivity studies suggest that the water content of the transition zone might be highly variable, ranging from <0.1 to 0.2% wt% water (Huang et al., 2005; Yoshino et al., 2008; Karato, 2011) in the Central Pacific to as much as 0.5–1 wt% water in the transition zone beneath subduction zone such as beneath Eastern Asia (Kelbert et al., 2009). Based on basalt geochemistry Kuritani et al. (2011) suggested that beneath Northeast China intensive hydration occurred more than one billion years ago in the transition zone as a result of dehydration of a subducted slab. Khan and Shankland (2012) combined the laboratory-based electrical conductivity measurements with electromagnetic sounding methods to constrain the water content for Earth's mantle and suggested that water content in the transition zone depends more on the choice of conductivity data set used. For example, using Yoshino and Katsura (2009) database shows "wet" transition zone which results in localized thin melt layers above the transition zone whereas using Karato and Dai (2009) dataset implies relatively "dry" transition zone and no melt layers. Recent seismological observations using receiver functions beneath the Ethiopian rift suggest that the depth of the 660 km discontinuity varies by 30–40 km (Cornwell et al., 2011), which is interpreted as a variation in the chemical composition of the mantle transition zone between olivine and a piclogitic piles (mainly made up of clinopyroxene and garnet). The Earth's mantle is heterogeneous, which is associated with depletion of the continental lithospheric mantle. Several locations at the base of the transition zone near 660 km depth are enriched in harzburgite component (Fukao et al., 2001; Cammarano et al., 2005; Nakagawa and Buffett, 2005; Hetényi et al., 2009). In the present study, the effect of water on 660 km discontinuity is large for Mg_2SiO_4 compared to hydrous pyrolite (Litasov et al., 2005b). Our hydrous Mg_2SiO_4 composition is close to Fe depleted harzburgitic composition containing small amount of Al and Ca (~1 wt%) compared to 4–5 wt% Al and 3–4 wt% Ca in pyrolite. Furthermore, harzburgite and pyrolite contain up to 8 wt% Fe, although Al has a stronger effect on the PST compared to Fe mainly because of substitution of Si by Al+H in the octahedral site in lower mantle phases (Panero and Stixrude, 2004; Litasov et al., 2007). Our results suggest that such a wide variability in water content should dominate the variation in depth of the 660 km seismic discontinuity, with over 30 km depth variation due to water alone. One place where the 660 km discontinuity appears to be anomalously deep, at 690 km, is beneath the Indian Ocean (Deuss et al., 2006). Since there is no fast seismic anomaly in the transition zone beneath the Indian Ocean (*e.g.* Romanowicz, 2008) we can rule out the effect of temperature in this region and we tentatively suggest that this might be a region where the mantle transition zone is strongly hydrated.

Acknowledgments

We thank H. Terasaki, Y. Shibazaki, S. Ozawa, T. Sakamaki, H. Hayashi and K. Nishida for their technical help at 'SPring-8'. We greatly appreciate the discussion and suggestions by Tomo Katsura

which improved the quality of the manuscript. We thank György Hetényi for various discussions on geophysical aspects on the current project. We also thank two anonymous reviewers for constructive reviews. The experiments were conducted when S.G. was at Tohoku University, while most of the manuscript was written while S.G. was at ETH Zurich. S.G. gratefully acknowledges the Ministry of Education, Culture, Science, Sport and Technology, Japan for providing him the Monbukagakusho Fellowship. This work was supported by the Grants-in-aid for Scientific Research from Ministry of Education, Culture, Science, Sport and Technology of Japanese Government (Nos. 18104009 and 22000002) to E.O., and conducted as a part of the 21st Century-of-Excellence program, 'Advanced Science and Technology Center for the Dynamic Earth' and Global Center of Excellence program, 'Global Education and Research Center for the Earth and Planetary Dynamics' at Tohoku University. At ETH Zurich, S.G. was supported by a SNF grant (# 200020-130100/1) which is gratefully acknowledged.

Appendix A. Supplementary material

Supplementary data associated with this article can be found in the online version at http://dx.doi.org/10.1016/j.epsl.2013.04.011.

References

Akaogi, M., Ito, E., Navrotsky, A., 1989. Olivine-modified spinel–spinel transition in the system Mg_2SiO_4–Fe_2SiO_4 calorimetric measurements, thermochemical calculation, and geophysical application. J. Geophys. Res. 94, 15671–15685.

Akaogi, M., Kojitani, H., Matsuzaka, K., Suzuki, T., Ito, E., 1998. Postspinel transformations in the system Mg2SiO4-Fe2SiO4 element partitioning, calorimetry, and thermodynamic calculation. In: Properties of Earth and Planetary Materials at High Pressure and Temperature, Geophys. Monogr. Ser., vol. 101. Washington, DC. pp. 373–384, AGU, doi:10.1029/GM101p0373.

Anderson, O.L., Issak, D.G., Yamamoto, S., 1989. Anharmonicity and the equation of state for gold. J. Appl. Phys. 65, 1534–1543.

Andrews, J., Deuss, A., 2008. Detailed nature of the 660 km region of the mantle from global receiver function data. J. Geophys. Res. 113 (B6), B06304.

Benz, H.M., Vidale, J.E., 1993. Sharpness of upper-mantle discontinuities determined from high-frequency reflections. Nature 365, 147–150.

Bercovici, D., Karato, S., 2003. Whole-mantle convection and the transition zone water filter. Nature 425, 39–44.

Bina, C.R., Helffrich, G.R., 1994. Phase transition Clapeyron slopes and transition zone seismic discontinuity topography. J. Geophys. Res. 99, 5853–15860.

Bolfan-Casanova, N., Keppler, H., Rubie, D.C., 2000. Water partitioning between nominally anhydrous minerals in the MgO–SiO_2–H_2O system up to 24 GPa: implications for the distribution of water in the Earth's mantle. Earth Planet. Sci. Lett. 182, 209–221.

Bolfan-Casanova, N., Keppler, H., Rubie, D.C., 2003. Water partitioning at 660 km depth and evidence for very low water solubility in magnesium silicate perovskites. Geophys. Res. Lett. 30, 1905, http://dx.doi.org/10.1029/2003GL017182.

Bolfan-Casanova, N., Mackwell, S., Keppler, H., McCammon, C., Rubie, D.C., 2002. Pressure dependence of H solubility in magnesiowustite up to 25 GPa: implications for the storage of water in the Earth's lower mantle. Geophys. Res. Lett. 29, 1449.

Cammarano, F., Goes, S., Deuss, A., Giardini, D., 2005. Is a pyrolitic adiabatic mantle compatible with seismic data? Earth Planet. Sci. Lett 232, 227–243.

Chen, J., Inoue, T., Weidner, D.J., Wu, Y., Vaughan, M.T., 1998. Strength and water weakening of mantle minerals, olivine, wadsleyite and ringwoodite. Geophys. Res. Lett. 25, 575–578.

Christensen, U.R., 1995. Effects of phase transitions on mantle convection. Annu. Rev. Earth Planet. Sci. 23, 65–87.

Chudinovskikh, L., Boehler, R., 2001. High-pressure polymorphs of olivine and the 660-km seismic discontinuity. Nature 411, 574–577.

Cornwell, D.G., Hetényi, G., Blanchard, T.D., 2011. Mantle transition zone variations beneath the Ethiopian rift and Afar: chemical heterogeneity within a hot mantle? Geophys. Res. Lett. 38, L16308, http://dx.doi.org/10.1029/2011GL047575.

Deuss, A., Redfern, S.A.T., Chambers, K., Woodhouse, J.H., 2006. The nature of the 660-kilometer discontinuity in Earth's mantle from global seismic observations of PP precursors. Science 311, 198–201.

Dziewonski, A.M., Anderson, D.L., 1981. Preliminary reference Earth model. Phys. Earth Planet. Inter. 25, 297–356.

Fei, Y., Li, J., Hirose, K., Minarik, W., Van Orman, J., Sanloup, C., van Westrenen, W., Komabayashi, T., Funakoshi, K., 2004a. A critical evaluation of pressure scales at high temperatures by *in situ* X-ray diffraction measurements. Phys. Earth Planet. Inter. 143/144, 516–526.

Fei, Y., Van Orman, J., Li, J., van Westrenen, W., Sanloup, C., Minarik, W., Hirose, K., Komabayashi, T., Walter, M., Funakoshi, K., 2004b. Experimentally determined postspinel transformation boundary in Mg_2SiO_4 using MgO as an internal pressure standard and its geophysical implications. J. Geophys. Res. 109, B02305, http://dx.doi.org/10.1029/2003JB002562.

Flanagan, M.P., Shearer, P.M., 1998. Global mapping of topography on transition zone velocity discontinuities by stacking SS precursors. J. Geophys. Res. 103, 2673–2692.

Fukao, Y., Obayashi, M., Nakakuki, T., 2009. the Deep Slab Project Group, 2009. Stagnant slab: a review. Annu. Rev. Earth Planet. Sci. 37, 10.1–10.28.

Fukao, Y., Widiyantoro, S., Obayashi, M., 2001. Stagnant slabs in the upper and lower mantle transition region. Rev. Geophys. 39, 291–323.

Green, D.H, Ringwood, A.E., 1967. The stability fields of alumious pyroxene peridotite and garnet peridotite and their relevance in upper mantle structure. Earth Planet. Sci. Lett. 3, 151–160.

Gu, Y.J., Dziewonski, A.M., 2002. Global variability of transition zone thickness. J. Geophys. Res. 107 (B7), http://dx.doi.org/10/1029/2001JB000489.

Helffrich, G.R., 2000. Topography of the transition zone seismic discontinuities. Rev. Geophys. 38, 141–158.

Hetényi, G., Stuart, G.W., Houseman, G.A., Horváth, F., Hegedus, E., Brückl, E., 2009. Anomalously deep mantle transition zone below Central Europe: evidence of lithospheric instability. Geophys. Res. Lett. 36, L21307, http://dx.doi.org/10.1029/2009GL040171.

Higo, Y., Inoue, T., Irifune, T., Yurimoto, H., 2001. Effect of water on the spinel–postspinel transformation in Mg_2SiO_4. Geophys. Res. Lett. 28, 3505–3508.

Hirschmann, M.M., 2006. Water, melting, and the deep Earth H_2O cycle. Annu. Rev. Earth Planet. Sci. 34, 629–653.

Hofmann, A.W., 1997. Mantle geochemistry: the message from oceanic volcanism. Nature 385, 219–229.

Huang, X., Xu, Y., Karato, S., 2005. Water content of the mantle transition zone from the electrical conductivity of wadsleyite and ringwoodite. Nature 434, 746–749.

Irifune, T., Nishiyama, N., Kuroda, K., Inoue, T., Isshiki, M., Utsumi, W., Funakoshi, K., Urakawa, S., Uchida, T., Katsura, T., Ohtaka, O., 1998. The postspinel phase boundary in Mg_2SiO_4 determined by *in situ* X-ray diffraction. Science 279, 1698–1700.

Ishii, T., Kojitani, H., Akaogi, M., 2011. Post-spinel transitions in pyrolite and Mg_2SiO_4 and akimotoite-perovskite transition in $MgSiO_3$: precise comparison by high-pressure high-temperature experiments with multi-sample cell technique. Earth Planet. Sci. Lett. 309, 185–197.

Ita, J., Stixrude, L., 1992. Petrology, elasticity, and composition of the mantle transition zone. J. Geophys. Res. 97, 6849–6866.

Ito, E., Takahashi, E., 1989. Post-spinel transformation in the system Mg_2SiO_4–Fe_2SiO_4 and some geophysical implications. J. Geophys. Res. 94, 10637–10646.

Khan, A., Shankland, T.J., 2012. A geophysical perspective on mantle water content and melting: inverting electromagnetic sounding data using laboratory-based electrical conductivity profiles. Earth Planet. Sci. Lett. 317–318, 27–43.

Karato, S., 2006. Influence of hydrogen-related defects on the electrical conductivity and plastic deformation of mantle minerals: a critical review. In: Jacobsen, S.D., van der Lee, S. (Eds.), Earth's Deep Water Cycle. AGU, Washington, DC, pp. 113–129.

Karato, S., 2011. Water distribution across the mantle transition zone and its implications for global material circulation. Earth Planet. Sci. Lett. 301, 413–423.

Karato, S., Dai, L., 2009. Comments on "Electrical conductivity of wadsleyite as a function of temperature and water content" by Manthilake et al. Phys. Earth Planet. Inter. 174, 19–21.

Katsura, T., Yamada, H., Kubo, A., Shinmei, T., Nishikawa, O., Yoshino, T., Aizawa, Y., Song, M.-s., Walter, M.J., Ito, E., Funakoshi, K., 2004a. Olivine–wadsleyite transition in the system $(Mg,Fe)_2SiO_4$. J. Geophys. Res. 109, B02209, http://dx.doi.org/10.1029/2003JB002438.

Katsura, T., Yamada, H., Shinmei, T., Kubo, A., Ono, S., Kanzaki, M., Yoneda, A., Walter, M.J., Ito, E., Urakawa, S., Funakoshi, K., Utsumi, W., 2003. Post-spinel transition in Mg_2SiO_4 determined by high P–T *in situ* X-ray diffraction. Phys. Earth Planet. Inter. 136, 11–24.

Katsura, T., Yokoshi, S., Song, M.-S., Kawabe, K., Tsujimura, T., Kubo, A., Ito, E., Tange, Y.Tomioka, Keiko, N., S, Funakoshi, K., 2004b. Thermal expansion of Mg_2SiO_4 ringwoodite at high pressures. J. Geophys. Res. B 109, B12209.

Katsura, T., Yoneda, A., Yamazaki, D., Yoshino, T., Ito, E., 2010. Adiabatic temperature profile in the mantle. Phys. Earth Planet. Inter. 183, 212–218.

Kelbert, A., Schultz, A., Egbert, G., 2009. Global electromagnetic induction constraints on transition-zone water content variations. Nature 460, 1003–1006.

Kohlstedt, D.L., Keppler, H., Rubie, D.C., 1996. Solubility of water in the α, β, and γ phases of $(Mg,Fe)_2SiO_4$. Contrib. Miner. Petrol. 123, 345–357.

Kubo, T., Ohtani, E., Kato, T., Urakawa, S., Suzuki, A., Kanbe, Y., Funakoshi, K.I., Utsumi, W., Kikegawa, T., Fujino, K., 2002. Mechanisms and kinetics of the post-spinel transformation in Mg2SiO4. Phys. Earth Planet. Inter. 129, 153–171.

Kuritani, T., Ohtani, E., Kimura, J., 2011. Intensive hydration of the mantle transition zone beneath China caused by ancient slab stagnation. Nat. Geosci. 4, 713–716.

Lebedev, S., Chevrot, S., van der Hilst, R.D., 2002. Seismic evidence for olivine phase changes at the 410- and 660-kilometer discontinuities. Science 296, 1300–1302.

Li, X.Q., Yuan, X.H., 2003. Receiver functions in northeast China — implications for slab penetration into the lower mantle in northwest Pacific subduction zone. Earth Planet. Sci. Lett 216, 679–691.

Litasov, K., Ohtani, E., Langenhorst, F., Yurimoto, H., Kubo, T., Kondo, T., 2003. Water solubility in Mg-perovskites, and water storage capacity in the lower mantle. Earth Planet. Sci. Lett. 211, 189–203.

Litasov, K.D., 2010. The influence of Al_2O_3 on the H_2O content in periclase and ferropericlase at 25 GPa. Russ. Geol. Geophys. 51, 644–649.
Litasov, K.D., Ohtani, E., 2007. Effect of water on the phase relations in Earth's mantle and deep water cycle. Geol. Soc. Am. Spec. Pap. 421, 115–156.
Litasov, K.D., Ohtani, E., Sano, A., Suzuki, A., Funakoshi, K., 2005a. In situ X-ray diffraction study of post-spinel transformation in a peridotite mantle: implication to the 660-km discontinuity. Earth Planet. Sci. Lett. 238, 311–328.
Li, X.Y., Jeanloz, R., 1987. Electrical conductivity of (Mg,Fe)SiO3 perovskite and a perovskite-dominated assemblage at lower mantle conditions. Geophys. Res. Lett. 14, 1075–1078.
Litasov, K.D., Ohtani, E., Sano, A., Suzuki, A., Funakoshi, K., 2005b. Wet subduction versus cold subduction. Geophys. Res. Lett. 32, L13312, http://dx.doi.org/10.1029/2005GL022921.
Litasov, K.D., Kagi, H., Shatskly, A., Ohtani, E., Lakshtanov, D.L., Bass, J.D., Ito, E., 2007. High hydrogen solubility in A1-rich stishovite and water transport in the lower mantle. Earth Planet. Sci. Lett. 262, 620–634.
Liu, L.G., 1976. The post-spinel phases of forsterite. Nature 262, 770–772.
Lombardi, D., Braunmiller, J., Kissling, E., Giardini, D., 2009. Alpine mantle transition zone imaged by receiver functions. Earth Planet. Sci. Lett 278, 163–174.
Nakagawa, T., Buffett, B.A., 2005. Mass transport mechanism between the upper and lower mantle in numerical simulations of thermochemical mantle convection with multicomponent phase changes. Earth Planet. Sci. Lett. 230, 11–27.
Ohtani, E., Litasov, K.D., 2006. The effect of water on mantle phase transition. Rev. Mineral. Geochem. 62, 397–420.
Ohtani, E., Mizobata, H., Yurimoto, H., 2000. Stability of dense hydrous magnesium silicate phases in the system Mg_2SiO_4–H_2O and $MgSiO_3$–H_2O at pressures up to 27 GPa. Phys. Chem. Miner. 27, 533–544.
Ohtani, E., 2005. Effect of water on phase transitions in the Earth's mantle. Element 1, 25–30.
Ohtani, E., Litasov, K., Hosoya, T., Kubo, T., Kondo, T., 2004. Water transport into the deep mantle and formation of a hydrous transition zone. Phys. Earth Planet. Inter. 143–144, 255–269.
Panero, W.R., Stixrude, L.P., 2004. Hydrogen incorporation in stishovite at high pressure and symmetric hydrogen bonding in delta-AlOOH. Earth Planet. Sci. Lett. 221, 421–431.
Petersen, N., Gossler, J., Kind, R., Stammler, K., Vinnik, L., 1993. Precursors to SS and structure of transition zone of the North-Western Pacific. Geophy. Res. Lett 20, 281–284.
Ringwood, A.E., 1975. Composition and Petrology of the Earth's Mantle. McGraw-Hill, New York630.
Romanowicz, B., 2008. Using seismic waves to image Earth's internal structure. Nature 451 (7176), 266–268.
Schubert, G., Turcotte, D.L., Olsen, P., 2001. Mantle Convection in the Earth and Planets. Cambridge University Press, Cambridge, U.K..
Shearer, P.M., 2000. Upper mantle seismic discontinuities. In: Earth's Deep Interior: Mineral Physics and Tomography From the Atomic to the Global Scale, Geophys. Monogr. Ser., vol. 117. Washington, D. C., pp. 115–131, AGU, http://dx.doi.org/10.1029/GM117p0115.
Shim, S.H., Duffy, T.S., Shen, G., 2001. The post-spinel transformation in Mg_2SiO_4 and its relation to the 660-km seismic discontinuity. Nature 411, 571–574.
Smyth, J.R., Holl, C.M., Frost, D.J., Jacobsen, S.D., Langenhorst, F., McCammon, C.A., 2003. Structural systematics of hydrous ringwoodite and water in Earth's interior. Am. Mineral. 88, 1402–1407.
Speziale, S., Zha, C.S., Duffy, T.S., Hemley, R.J., Mao, H.K., 2001. Quasi-hydrostatic compression of magnesium oxide to 52 GPa: implications for the pressure–volume–temperature equation of state. J. Geophys. Res. 106, 515–528.
Tackley, P.J., Stevenson, D.J., Glatzmaier, G.A., Schubert, G., 1993. Effects of an endothermic phase transition at 670-km depth in a spherical model of convection in the Earth's mantle. Nature 361, 699–704.
Tsuchiya, T., 2003. First-principles prediction of the P–V–T equation of state of gold and the 660-km discontinuity in Earth's mantle. J. Geophys. Res. 108, 2462, http://dx.doi.org/10.1029/2003JB002446 , B10.
Wang, B., Niu, F., 2010. A broad. 660 km discontinuity beneath northeast China revealed by dense regional seismic networks in China. J. Geophys. Res. 115, http://dx.doi.org/10.1029/2009JB006608.
Weidner, D.J., Wang, Y., 1998. Chemical- and Clapeyron-induced buoyancy at the 660 km discontinuity. J. Geophys. Res. 103, 7431–7441.
Wood, B.J., 1995. The effect of H_2O on the 410-kilometer seismic discontinuity. Science 268, 74–76.
Wood, B.J., Rubie, D.C., 1996. The effect of alumina on phase transformations at the 660-kilometer discontinuity from Fe–Mg partitioning experiments. Science 273, 1522–1524.
Yamazaki, A., Hirahara, K., 1994. The thickness of upper mantle discontinuities as inferred from short-period J-array data. Geophys. Res. Lett. 21, 1811–1814.
Yoshino, T., Katsura, T., 2009. Reply to comments on "Electrical conductivity of wadsleyite as a function of temperature and water content" by Manthilake et al. Phys. Earth Planet. Inter. 174, 22–23.
Yoshino, T., Manthilake, G., Matsuzaki, T., Katsura, T., 2008. Dry mantle transition zone inferred from the conductivity of wadsleyite and ringwoodite. Nature 451, 326–329.
Yu, Y.G., Wentzcovitch, R.M., Tsuchiya, T., Umemoto, K., Weidner, D.J., 2007. First principles investigation of the postspinel transition in Mg_2SiO_4. Geophys. Res. Lett. 34, L10306, http://dx.doi.org/10.1029/2007GL029462.